



## Optimization Ground Glass Opacities (GGO) Detection Using Multipixel Interpolation Techniques

Musli Yanto<sup>1</sup>, Yogi Wiyandra<sup>2</sup>

<sup>1,2</sup>Teknologi Informasi, Fakultas Ilmu Komputer, Universitas Putra Indonesia YPTK Padang  
[musli\\_yanto@upiypk.ac.id](mailto:musli_yanto@upiypk.ac.id)

### Abstract

Ground Glass Opacities (GGO) are a picture of abnormal lung conditions characterized by white or gray areas. This picture of GGO in the lungs could previously be detected based on the results of medical examinations such as Computerized Tomography (CT scan) and Magnetic Resonance Imaging (MRI) images of patients suffering from Covid-19. However, from the results of the examination, it can be seen that the CT scan and MRI images still have a noise level that is too high, causing difficulties in describing the distribution pattern of the GGO itself. The purpose of this study was to optimize the detection of GGO on MRI images using the Multipixel Interpolation technique. The detection process adopts several stages including image preprocessing, edge detection process, and gradient morphological segmentation. Image preprocessing is done to remove noise and improve the MRI input image. The edge detection process is carried out to detect lung organs automatically using the Canny method which is optimized with the multipixel interpolation technique. The final stage of the research is the segmentation process using a gradient morphology technique to see the spread of GGO in patients with Covid-19 contained in the MRI image. The results of this study present an overview of the GGO pattern with fairly good results. The results of the GGO pattern description will also measure the level of spread to see the severity of pneumonia. Based on the results presented, this research is useful as an alternative solution in the process of diagnosis and treatment of Covid-19 patients.

**Keywords:** Computerized Tomography (CT scan), Magnetic Resonance Imaging (MRI), Multipixel Interpolation Technique, Ground Glass Opacities (GGO), Covid-19

### 1. Introduction

Ground-glass opacity (GGO) is one of the findings of diseases that cause inflammation of the lungs [1]. Basically, the proportion of patients with pneumonia can be described based on the spread of the GGO pattern [2]. GGO can indicate a pre-invasive lung area with white and gray patches appearing around the lung [3]. Based on this, the effect of GGO will cause severe damage to the lungs so performance will not function optimally [4]. Not only that, but persistent GGO can also lead to early-stage lung cancer [5].

The spread of GGO can be seen with medical images to describe lung conditions [6]. Medical images have played an active role in supporting activities to solve existing problems [7]. Medical image is basically a medical diagnostic technology that can be implemented according to the needs in diagnosing a disease [8]. The previous explanation explained that medical imaging is a tool used to carry out the disease detection process [9]. Diagnostic imaging technology provides early diagnosis of problematic medical conditions [10].

Problems that arise, medical technology is currently still undergoing development so the results presented cannot be optimal [11]. To overcome these problems, development is needed that is able to support and promise a far significant impact in the medical world [12]. The development carried out aims to be able to overcome the difficulties of problems in the medical field in a solution that can be adopted by medical parties in the future [13].

One of the developments in medical technology can be seen in the performance of Artificial Intelligence (AI) which drives change optimally [14]. Advances in artificial intelligence (AI) technology have brought major changes and impacts in the medical field [15]. The performance of AI in medicine can be presented in the form of Digital Image Processing technology that has been able to handle problems [16]. The development of DIP is able to provide maximum performance of medical technology in the diagnostic process [17]. The role of DIP is to overcome the

problems of medical technology by providing better anti-noise capabilities [18].

The problem in the GGO diagnosis process was initially carried out by presenting fairly good results with an accuracy of 90.83% and an average precision of 0.905 [19]. Furthermore, other studies have also explained that DIP is able to produce a model for identifying lung damage due to COVID-19 based on the description of the GGO pattern [20]. DIP can also be used as a useful tool for clinical practitioners and radiologists in the process of diagnosis, quantification, and follow-up in handling COVID-19 cases [21].

The application of DIP can be seen based on the identification and diagnosis process by adopting image segmentation techniques [22]. The segmentation technique is a technique that has been widely used to separate an object in the image [23]. Segmentation works optimally which can be used as a basis in a process of diagnosing a disease [24]. Image segmentation detects objects with edge detection and shows good results in identifying an object in the image [25]. The results presented are also able to provide an efficient presentation in supporting decision-making [26].

Basically, the segmentation process has developed with the algorithm model that has been generated in the detection process. One of the techniques used is the Interpolation technique. This technique is an important process used in image processing and computer graphics in wide applications for medical imaging [27]. The interpolation technique works by recovering images and animations that have noise [28]. The implementation of the interpolation technique provides a better compression rate and reconstruction quality with an accuracy of 92.12% in the image classification process [29].

Previous research in the process of diagnosing GGO using the image segmentation process gave quite effective results in helping medical parties deal with the problems of Covid-19 patients [30]. The segmentation technique automatically is also able to produce a model for handling COVID cases efficiently with an accuracy of 0.8069, specificity of 0.9969, and sensitivity of 0.8354 [31]. The segmentation results provide excellent performance results of several previously proposed model frameworks with an average precision level of 90.23% [32]. The same study also explained that the manual segmentation process of 3 labels: normal lung, ground-glass opacity (GGO), and consolidation (Cons) presented the performance of the model evaluated with technical metrics, volume, and area with a fairly good level of accuracy [33].

An automated segmentation approach to determine gross GGO volume in computed tomography (CT) images gave an accuracy of 0.838 [34]. Research with the proposed convolution model accurately classifies nodules on GGO objects using multiscale feature aggregation and downsampling approach [35]. The semantic segmentation of the ground-glass opacity (GGO) area on Computer Tomography (CT) scan images of patients affected by COVID-19 can provide a fairly good level of diagnostic accuracy [36].

Based on previous research on the problem of the GGO diagnosis process, this study will also adopt a detection process using image segmentation techniques. The segmentation process was developed using Multipixel Interpolation (IM). The development of the segmentation process can provide optimal detection results in describing the distribution pattern of GGO on Magnetic Resonance Imaging (MRI) images. Overall, this study presents an update on the segmentation algorithm developed using the multi-pixel interpolation technique. The newest segmentation algorithm is presented in the morphological operation process in detecting GGO image objects. The results of the study will present a model for the detection of GGO to support medical performance in treating patients. The research contribution will have an impact on the image segmentation process to provide optimal results.

## 2. Research Methods

The process of detecting GGO is carried out by adopting the IM technique on MRI images. The process is presented in the form of process steps that are carried out starting from the image convention process, image preprocessing, the image edge detection process, and segmentation of the GGO distribution pattern. The conversion process is carried out to make changes to the images of medical examination results on MRI images. After the conversion process is carried out, the process is continued at the image preprocessing stage to ensure that the MRI images have good enough quality in the detection process. The detection process begins by detecting the lungs using edge detection techniques. After the lungs are detected, the process is continued at the stage of detecting GGO using segmentation techniques. The segmentation process uses optimized morphological operations with multi-pixel interpolation techniques. The results presented from the process will be able to clearly describe the GGO object accompanied by accurate information from the spread of the GGO pattern. All stages of the process will be carried out using the Matlab 2018a software tool. as for the presentation of the process in this study can be seen in Figure 1.

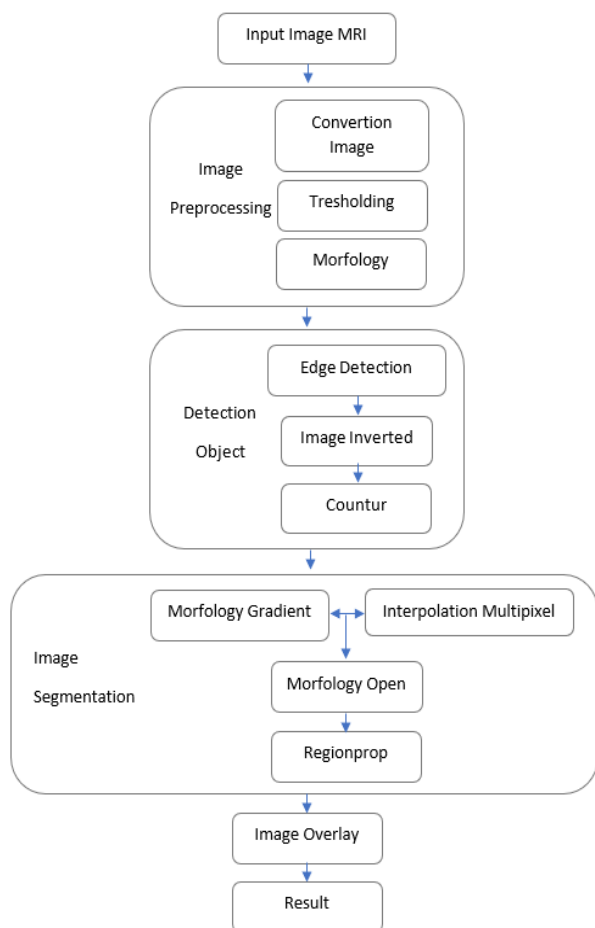


Figure 1. Stages of the Ground Glass Opacities (GGO) Detection Process

Figure 1 describes the stages of the process carried out in the detection of GGO. These stages are presented in three stages. These stages include:

### A. Image Preprocessing

This stage is carried out to clean the image from noise contained in the MRI image. The image improvement process begins by converting images from RGB (Red Green Blue) images to gray images and binary images. After the conversion process is carried out the preprocessing stage is continued at the filtering stage using thresholding techniques on binary images. The final process of the preprocessing stage is carried out using open morphology techniques to remove noise objects in the image. After the preprocessing results present a better image in the GGO detection process.

### B. Detection Object

This object detection stage is carried out using edge detection techniques. The edge detection used is using the canny command to obtain an image of the lung object. The canny command in the edge detection process can perform optimal detection to provide clarity of the detected lung organs. After the edge detection

process is carried out, the steps are continued at the image inverted stage. This stage is done to get the organ to be detected. After the image of the lung, object has been obtained, the process is continued to perform contouring on the object of the lung image. The results of image contouring will present image output that can clearly describe the condition of the lungs identified by GGO.

### C. Image Segmentation

The image segmentation process is the stage used to detect the part of the GGO object in the lungs. The process carried out is segmentation using a gradient morphology technique by adopting a multipixel interpolation technique. The results of this process provide an accurate description of the GGO detection process. After the gradient morphology process is carried out, the process continues by using open morphology to separate lung objects from GGO objects and this stage will end by calculating the amount of GGO objects detected using regionprop. The results of image segmentation will present an image by displaying information about the identified GGO objects.

#### 2.1 Edge Detection

Edge detection is one of the techniques interested in an image in recognizing objects with edges contained in the image [37]. Edge detection is also a process of forming an object [38]. The purpose of edge detection operation is to improve the appearance of the boundary line of an area or object in the image [39]. The operation used in conducting the edge detection process in this study uses the canny operator. The form of the canny operator matrix can be presented in Figure 2 [40].

$C_x$	1	0	-1	$C_y$	-1	-1	-1
	1	0	-1		0	0	0
	1	0	-1		1	1	1

Figure. 2 Canny Matrix Operators

Figure 2 is a canny operator matrix with a 3x3 matrix. Edge detection is done by reading each pixel in the image by taking the upper leftmost pixel (northeast) and moving to the bottom rightmost pixel (southwest). Edge tracing,  $G_x$ , and  $G_y$  gradients are calculated by matrix [40].

#### 2.2 Morphological Gradient

The morphological gradient is a process of drawing objects in the image to clarify the edges of each object [41]. Gradient morphology can also be called edge image because with the performance of this technique it can reduce the results of the thickening and thinning operation of the image that accentuates the edges of the object [42]. Morphological operations are operations that are commonly used to change the shape of objects contained in the image [43].

### 2.3 Multipixel Interpolation

Interpolation operation is a process used in increasing the image size by reducing the size first [44]. Image interpolation techniques are often required in medical imaging for image generation and such as compression or sampling of objects from an image [45]. Analyzing interpolation techniques have been applied to find various interpolation schemes in medical imaging images [46]. The form of the performance process of multi-pixel interpolation can be seen in Figure 3 [47].

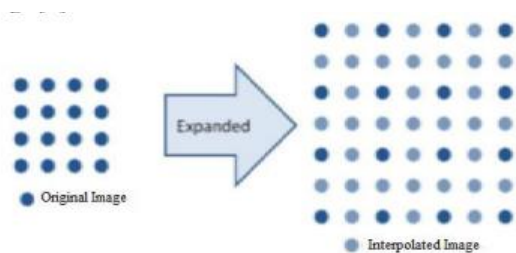


Figure. 3 Image Interpolation Matrix

Figure 3 describes the process of an interpolation technique based on direct utilization of the pixels of an

image. The process is done by considering the features or objects of an image. These techniques follow the same pattern for all pixels [47].

### 3. Results and Discussions

The discussion in the GGO detection process begins with the preprocessing process. The intended result of this process is to get a better image that will be used in diagnosis. The preprocessing process is carried out using thresholding techniques and the morphology of the opening operation. The thresholding technique is used to provide output in the form of a binary image by ensuring the threshold value of the object is detected. The thresholding process is carried out automatically based on the threshold value obtained. Morphological operations with opening operations are used to give a magnifying effect to the segmented object. The results of the opening morphology will provide clarity in separating the lung organs in the detection of GGO objects. The preprocessing results produced can be presented in Table 1.

Table. 1 Image Preprocessing Results

No	No. Pasien	Image Input	Thresholding Result	Morfology Result
1	P-001			
2	P-002			
3	P-003			
4	P-004			
5	P-005			

Table 1 presents the results of image preprocessing in patients indicated by GGO. The results of preprocessing provide good image improvement results for the GGO detection process. After the preprocessing process, the process continues to perform edge detection on the

object image. The operation used in edge detection uses the Canny operation. After the edge detection process, the inverted image process is carried out to provide the results of the detection process. The detection results can be presented in Table 2.

Table. 2 Edge Detection Results

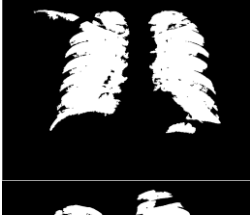
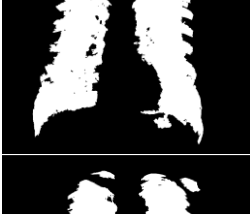
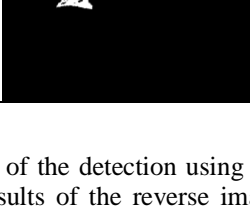
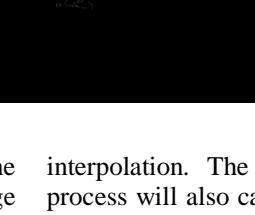
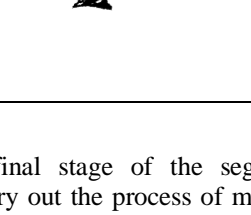
No	No. Pasien	Preprocessing Result	Edge Detection	Inverted Image
1	P-001			
2	P-002			
3	P-003			
4	P-004			
5	P-005			

Table 2 presents the results of the detection using the canny operation and the results of the reverse image process. After the detection process, it is continued to do segmentation using a gradient morphology technique that is optimized with multi-pixel

interpolation. The final stage of the segmentation process will also carry out the process of merging the input image with the detected GGO object using the image overlay command. The results of segmentation can be presented in Table 3.

Table. 3 Segmentation Results with Multipixel Interpolation Optimization

No	No. Pasien	Segmentation GGO Result	Detection GGO Result
1	P-001		

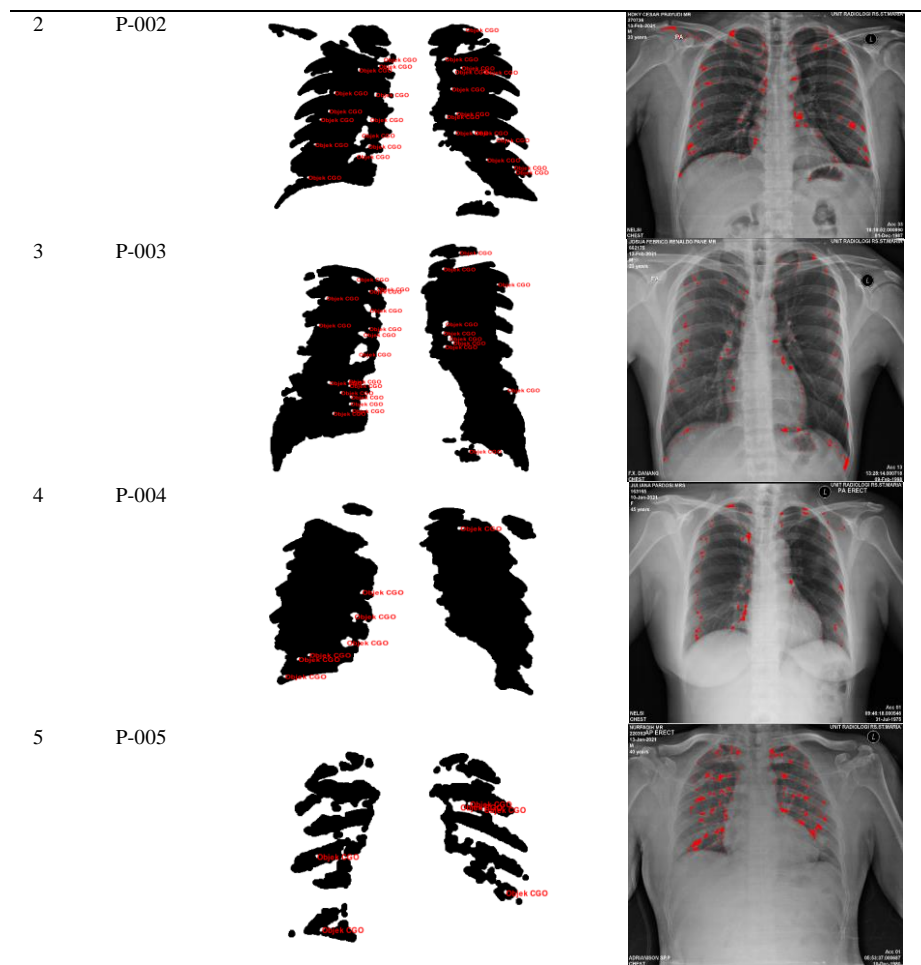


Table 3 presents the results of the segmentation process by displaying the detected GGO objects. Results Based on what is presented, the segmentation process using the multipixel interpolation technique provides optimal results in describing GGO objects. The results of the detection will be tested to measure the severity of the lung condition with the detected GGO object. The measurement process can be carried out using Equation 1 [20].

$$\text{Ratio}\% = \frac{\text{GGO Area}}{\text{Thorax Area}} \times 100\% \quad (1)$$

Equation 1 is a calculation used to measure the ratio of severity in the lungs that occurs from the pattern of spread of GGO. The rate ratio was measured by comparing the GGO area to the lung area. The results obtained will increase the severity level so that these results can be used as a basis for decision-making. The measurement results can be presented in Table 4.

Table 4 Measurement of Lung Severity Ratio Due to GGO

No	No. Pasien	Area Thorax	Area GGO	Ratio
1	P-001	4700	323955	1,45%
2	P-002	9671	493319	1,96%
3	P-003	18271	645186	2,83%
4	P-004	3310	381371	0,86%
5	P-005	3249	127635	2,54%

Table 4 presents the results of measuring the ratio of lung severity due to the pattern of spread of GGO. The output results based on this segmentation process will be compared with the segmentation process without using interpolation techniques to see how far the techniques used provide optimal results. the comparison process will see the size of the detected GGO object. The comparison can be presented in Table 5.

Tabel. 5 Comparison of GGO Object Segmentation Results

No	No. Pasien	GGO Object	
		Morfology	Morfology and Interpolation
1	P-001	99	4700
2	P-002	55	9671
3	P-003	444	18271
4	P-004	195	3310
5	P-005	86	3249

Table 5 presents the comparison process to ensure that the multipixel interpolation performance has run optimally. The results presented are that GGO objects detected without using interpolation techniques have not been able to describe GGO objects optimally. To ensure the level of accuracy in detecting GGO objects using the morphological segmentation process and interpolation techniques, the precision level measurement process can use Equation 2 [48]:

$$\text{Accuracy} = \frac{TP+TN}{TP+TN+FP+FN} \times 100\% \quad (2)$$

$$\text{Precision} = \frac{TP}{FP+FN} \times 100\% \quad (3)$$

$$\text{Recall} = \frac{TP}{FP+FN} \times 100\% \quad (4)$$

The results are based on measurements using the above equation, the results of the detection process provide an accuracy rate of 98.07%, a precision of 98.11%, and a recall of 98.02%. These results can indicate that the segmentation process using the interpolation technique gives maximum results. that affect the level of measurement measuring the process can be seen from the performance of the interpolation technique able to describe the spread of the GGO output pattern of the resulting output. It can be seen based on Table 5 which states that the output of the model testing process that is built presents the results of the new research in the image object segmentation process. The segmentation process will provide optimal output in the assessment process. These results can also be used by medical personnel in determining the severity status based on the ratio value obtained. With the results obtained, the detection process can provide maximum results for the GGO diagnosis process.

Based on the detection process by segmenting which adopts the multi-pixel interpolation technique, it gives quite significant results based on the level of accuracy obtained. The development of the segmentation process is presented in a model developed for the detection of GGO. These results can contribute to the development of medical technology in handling Covid-19 patients.

#### 4. Conclusion

The detection of GGO by adopting the multi-pixel interpolation technique provides optimal results to describe the spread of GGO in the lungs of patients with Covid-19. The output of the detection process presents the level of accuracy based on the accuracy value of the ratio obtained. The detection success rate using segmentation techniques and multiple pixel interpolation gives an accuracy percentage of 98.07%. The success of this process is based on the interpolation technique that can maximize the segmentation process in describing the condition of the lungs that are ARF. The resulting segmentation results give a blow to the pattern of spread of GGO in the detected lung parts.

These results become a finding in the recent development of detection algorithms. In general, the results of the spread of the visible pattern can be seen in the severity of the lung with the resulting status information. Results Based on this research, it can be said that the GGO detection process using the multipixel interpolation technique can provide optimal results for the development of technology in the field of medical imagery. This research also produces models in

detection to assist medical parties in handling Covid-19 cases. Model development is also expected to be compared with several other techniques to perform the segmentation process. The comparison results can present new knowledge in the segmentation process in the future.

#### Reference

- [1] D. Cozzi *et al.*, "Ground-glass opacity (GGO): a review of the differential diagnosis in the era of COVID-19," *Jpn. J. Radiol.*, vol. 39, no. 8, pp. 721–732, 2021, doi: 10.1007/s11604-021-01120-w.
- [2] B. Cheng *et al.*, "The impact of postoperative EGFR-TKIs treatment on residual GGO lesions after resection for lung cancer," *Signal Transduct. Target. Ther.*, vol. 6, no. 1, pp. 4–6, 2021, doi: 10.1038/s41392-020-00452-9.
- [3] E. Herskovitz, C. Solomides, J. Barta, N. Evans III, and G. Kane, "Detection of lung carcinoma arising from ground glass opacities (GGO) after 5 years-A retrospective review," *Respir. Med.*, vol. 196, p. 106803, 2022.
- [4] H. Herath, G. Karunasena, and B. Madhusanka, "Early detection of COVID-19 pneumonia based on ground-glass opacity (GGO) features of computerized tomography (CT) angiography," in *5G IoT and Edge Computing for Smart Healthcare*, Elsevier, 2022, pp. 257–277.
- [5] F. FU, X. MA, Y. ZHANG, and H. CHEN, "Personalized treatment strategy for ground-glass opacity-featured lung cancer," *Chinese J. Clin. Thorac. Cardiovasc. Surg.*, pp. 1–10, 2022.
- [6] Z. Wu *et al.*, "Correlation between ground-glass opacity on pulmonary CT and the levels of inflammatory cytokines in patients with moderate-to-severe COVID-19 pneumonia," *Int. J. Med. Sci.*, vol. 18, no. 11, p. 2394, 2021.
- [7] X. Liu, L. Song, S. Liu, and Y. Zhang, "A review of deep-learning-based medical image segmentation methods," *Sustain.*, vol. 13, no. 3, pp. 1–29, 2021, doi: 10.3390/su13031224.
- [8] Y. Li, J. Zhao, Z. Lv, and J. Li, "Medical image fusion method by deep learning," *Int. J. Cogn. Comput. Eng.*, vol. 2, pp. 21–29, 2021.
- [9] P. Kora *et al.*, "Transfer learning techniques for medical image analysis: A review," *Biocybern. Biomed. Eng.*, 2021.
- [10] V. Muneeswaran, P. Nagaraj, and M. F. Ijaz, "An Articulated Learning Method Based on Optimization Approach for Gallbladder Segmentation from MRCP Images and an Effective IoT Based Recommendation Framework BT - Connected e-Health: Integrated IoT and Cloud Computing," S. Mishra, A. González-Briones, A. K. Bhoi, P. K. Mallick, and J. M. Corchado, Eds. Cham: Springer International Publishing, 2022, pp. 165–179.
- [11] A. Barragán-Montero *et al.*, "Artificial intelligence and machine learning for medical imaging: A technology review," *Phys. Medica*, vol. 83, pp. 242–256, 2021.
- [12] A. Avidan, C. Weissman, and R. Y. Zisk-Rony, "Interest in technology among medical students early in their clinical experience," *Int. J. Med. Inform.*, vol. 153, p. 104512, 2021.
- [13] Y. Cheng *et al.*, "Research on the smart medical system based on NB-IoT technology," *Mob. Inf. Syst.*, vol. 2021, 2021.
- [14] J. Xu and F. Noo, "Convex optimization algorithms in medical image reconstruction—in the age of AI," *Phys. Med. Biol.*, vol. 67, no. 7, p. 07TR01, 2022.
- [15] H. Chen and J. J. Y. Sung, "Potentials of AI in medical image analysis in Gastroenterology and Hepatology," *J. Gastroenterol. Hepatol.*, vol. 36, no. 1, pp. 31–38, 2021.
- [16] Y. Pourasad, R. Ranjbarzadeh, and A. Mardani, "A new algorithm for digital image encryption based on chaos theory," *Entropy*, vol. 23, no. 3, p. 341, 2021.
- [17] A. Valikhani, A. Jaber Jahromi, S. Pouyanfar, I. M. Mantawy, and A. Azizinamini, "Machine learning and image processing approaches for estimating concrete surface roughness using

- basic cameras,” *Comput. Civ. Infrastruct. Eng.*, vol. 36, no. 2, pp. 213–226, 2021, doi: 10.1111/mice.12605.
- [18] S. Teng, G. Chen, S. Wang, J. Zhang, and X. Sun, “Digital image correlation-based structural state detection through deep learning,” *Front. Struct. Civ. Eng.*, vol. 16, no. 1, pp. 45–56, 2022.
- [19] H. Herath *et al.*, “Deep learning approach to recognition of novel COVID-19 using CT scans and digital image processing,” 2021.
- [20] J. Na’am, F. S. Pranata, R. Hidayat, A. M. Adif, and E. Ellyzarti, “Automated Identification Model of Ground-Glass Opacity in CT-Scan Image by COVID-19,” *Int. J. Adv. Sci. Eng. Inf. Technol.*, vol. 11, no. 2, pp. 595–602, 2021, doi: 10.18517/ijaseit.11.2.14143.
- [21] M. A. Dwijaya, U. A. Ahmad, R. P. Wijayanto, and R. A. Nugrahaeni, “Model Design of the Image Recognition of Lung CT scan for COVID-19 Detection Using Artificial Neural Network,” *J. Nas. Tek. ELEKTRO*, pp. 21–28, 2022.
- [22] N. Paluru *et al.*, “Anam-Net: Anamorphic depth embedding-based lightweight CNN for segmentation of anomalies in COVID-19 chest CT images,” *IEEE Trans. Neural Networks Learn. Syst.*, vol. 32, no. 3, pp. 932–946, 2021.
- [23] M. X.-L. Foo *et al.*, “Interactive Segmentation for COVID-19 Infection Quantification on Longitudinal CT scans,” *arXiv Prepr. arXiv2110.00948*, 2021.
- [24] R. Biondi *et al.*, “Classification Performance for COVID Patient Prognosis from Automatic AI Segmentation—A Single-Center Study,” *Appl. Sci.*, vol. 11, no. 12, p. 5438, 2021.
- [25] S. Saifullah and A. P. Suryotomo, “Detection of Chicken Egg Embryos using BW Image Segmentation and Edge Detection Methods,” *J. RESTI (Rekayasa Sist. Dan Teknol. Informasi)*, vol. 5, no. 6, pp. 1062–1069, 2021.
- [26] S. Yin, H. Deng, Z. Xu, Q. Zhu, and J. Cheng, “SD-UNet: A Novel Segmentation Framework for CT Images of Lung Infections,” *Electronics*, vol. 11, no. 1, p. 130, 2022.
- [27] J. Tavooosi, C. Zhang, A. Mohammadzadeh, S. Mobayen, and A. H. Mosavi, “Medical Image Interpolation Using Recurrent Type-2 Fuzzy Neural Network,” *Front. Neuroinform.*, vol. 15, no. September, pp. 1–10, 2021, doi: 10.3389/fninf.2021.667375.
- [28] C. Jittawiriyankoon and V. Srisarkun, “Evaluation of color image interpolation based on incompressible navier stokes technique,” *Bull. Electr. Eng. Informatics*, vol. 10, no. 3, pp. 1634–1639, 2021, doi: 10.11591/eei.v10i3.1820.
- [29] R. S. Nair and S. Domnic, “Deep-learning with context sensitive quantization and interpolation for underwater image compression and quality image restoration,” *Int. J. Inf. Technol.*, 2022, doi: 10.1007/s41870-022-01020-w.
- [30] S. A. Banday, R. Nahvi, A. H. Mir, S. Khan, A. S. AlGhamdi, and S. S. Alshamrani, “Ground glass opacity detection and segmentation using CT images: an image statistics framework,” *IET Image Process.*, 2022.
- [31] N. Enshaei *et al.*, “COVID-rate: an automated framework for segmentation of COVID-19 lesions from chest CT images,” *Sci. Rep.*, vol. 12, no. 1, pp. 1–18, 2022.
- [32] F. Faruk, “RGU-Net: Residual Guided U-Net Architecture for Automated Segmentation of COVID-19 Anomalies Using CT Images,” in *2021 International Conference on Automation, Control and Mechatronics for Industry 4.0 (ACMI)*, 2021, pp. 1–6.
- [33] A. Bartoli *et al.*, “Value and prognostic impact of a deep learning segmentation model of COVID-19 lung lesions on low-dose chest CT,” *Res. Diagnostic Interv. Imaging*, vol. 1, p. 100003, 2022.
- [34] S. Shamim, M. J. Awan, A. Mohd Zain, U. Naseem, M. A. Mohammed, and B. Garcia-Zapirain, “Automatic COVID-19 Lung Infection Segmentation through Modified Unet Model,” *J. Healthc. Eng.*, vol. 2022, 2022.
- [35] S. A. Agnes and J. Anitha, “Efficient multiscale fully convolutional UNet model for segmentation of 3D lung nodule from CT image,” *J. Med. Imaging*, vol. 9, no. 5, p. 52402, 2022.
- [36] R. Biondi, N. Curti, E. Giampieri, and G. Castellani, “COVID-19 Lung Segmentation,” *J. Open Source Softw.*, vol. 6, no. 65, p. 3447, 2021.
- [37] Wicaksono Yuli Sulistyono, Imam Riadi, and Anton Yudhana, “Comparative Analysis of Image Quality Values on Edge Detection Methods,” *J. RESTI (Rekayasa Sist. dan Teknol. Informasi)*, vol. 4, no. 2, pp. 345–351, 2020, doi: 10.29207/resti.v4i2.1827.
- [38] M. Versaci and F. C. Morabito, “Image edge detection: A new approach based on fuzzy entropy and fuzzy divergence,” *Int. J. Fuzzy Syst.*, vol. 23, no. 4, pp. 918–936, 2021.
- [39] K. Letelay, “Perbandingan Kinerja Metode Deteksi Tepi,” *J-Icon*, vol. 7, no. 1, pp. 1–8, 2019.
- [40] A. Zalukhu, “Implementasi Metode Canny Dan Sobel Untuk Mendeteksi Tepi Citra,” *J. Ris. Komput.*, vol. 3, no. 6, pp. 25–29, 2016.
- [41] J. Na’am, J. Harlan, S. Madenda, and E. P. Wibowo, “Image processing of panoramic dental X-ray for identifying proximal caries,” *Telkomnika (Telecommunication Comput. Electron. Control)*, vol. 15, no. 2, pp. 702–708, 2017, doi: 10.12928/TELKOMNIKA.v15i2.4622.
- [42] A. Sutikno, E. Utami, and A. Sunyoto, “Penerapan metode morfologi gradien untuk perbaikan kualitas deteksi tepi pada citra motif batik,” *Respati*, vol. 9, no. 26, 2017.
- [43] O. Sihombing, E. Buulolo, H. K. Siburian, G. Batak, and M. O. Morfologis, “Hasil Segmentasi Citra Digital Gorga Batak,” *KOMIK (Konferensi Nas. Teknol. Inf. dan Komputer)*, vol. 2, pp. 40–48, 2018.
- [44] J. Tavooosi, C. Zhang, A. Mohammadzadeh, S. Mobayen, and A. H. Mosavi, “Medical image interpolation using recurrent type-2 fuzzy neural network,” *Front. Neuroinform.*, vol. 15, 2021.
- [45] T. M. Lehmann, C. Gonner, and K. Spitzer, “Survey: Interpolation methods in medical image processing,” *IEEE Trans. Med. Imaging*, vol. 18, no. 11, pp. 1049–1075, 1999.
- [46] T. M. Lehmann, C. Gonner, and K. Spitzer, “Addendum: B-spline interpolation in medical image processing,” *IEEE Trans. Med. Imaging*, vol. 20, no. 7, pp. 660–665, 2001.
- [47] V. Patel and K. Mistree, “A review on different image interpolation techniques for image enhancement,” *Ijetae*, vol. 3, no. 12, pp. 129–133, 2013, [Online]. Available: <http://citeseerx.ist.psu.edu/viewdoc/download?doi=10.1.1.638.313&rep=rep1&type=pdf>.
- [48] J. M. Apellániz, M. P. González, and R. H. Barbá, “Validation of the accuracy and precision of Gaia EDR3 parallaxes with globular clusters,” *Astron. Astrophys.*, vol. 649, p. A13, 2021.